© 2019. Published by The Company of Biologists Ltd | Journal of Experimental Biology (2019) 222, jeb199638. doi:10.1242/jeb.199638

RESEARCH ARTICLE

The gastric sieve of penaeid shrimp species is a sub-micrometer nutrient filter

Werawich Pattarayingsakul[1,2,*], Arnon Pudgerd[3,4,*], Natthinee Munkongwongsiri[5], Rapeepun Vanichviriyakit[2,3], Thawatchai Chaijarasphong[1,2], Siripong Thitamadee[1,2] and Thanapong Kruangkum[2,3,‡]

ABSTRACT

Unlike that of vertebrates, the penaeid shrimp stomach is of ectodermic origin and is thus covered by a cuticle that is sloughed upon molting. It is composed of two chambers, here called the anterior and posterior stomach chambers, ASC and PSC, respectively. The PSC contains a filtration structure variously called a pyloric filter, filter press, gastric filter or gastric sieve (GS), and the last of these will be used here. The GS resembles an elongated, inverted-V, dome-like, chitinous structure with a midline ridge that is integral to the ventral base of the PSC. The dome surface is covered with a carpet-like layer of minute, comb-like setae bearing laterally branching setulae. This carpet serves as a selective filter that excludes large partially digested food particles but allows smaller particles and soluble materials to enter hepatopancreatic ducts that conduct them into the shrimp hepatopancreas (HP), where further digestion and absorption of nutrients takes place. Although the GS function is well known, its exclusion limit for particulate material has not been clearly defined. Using histological and ultra-structure analysis, we show that the GS sieve pore diameter is approximately 0.2–0.7 µm in size, indicating a size exclusion limit of substantially less than 1 µm. Using fluorescent microbeads, we show that particles of 1 µm diameter could not pass through the GS but that particles of 0.1 µm diameter did pass through to accumulate in longitudinal grooves and move on to the HP, where some were internalized by tubule epithelial cells. We found no significant difference in these sizes between the species *Penaeus monodon* and *Penaeus vannamei* or between juveniles and adults in *P. vannamei*. This information will be of value for the design of particulate feed ingredients such as nutrients, therapeutic drugs and toxin-absorbing materials that may selectively target the stomach, intestine or HP of cultivated shrimp.

KEY WORDS: Alimentary tract, Stomach, *Penaeus monodon*, *Penaeus vannamei*, Fluorescent microbead, Sieve exclusion

[1]Department of Biotechnology, Faculty of Science, Mahidol University, Rama VI Rd, Bangkok 10400, Thailand. [2]Center of Excellence for Shrimp Molecular Biology and Biotechnology (Centex Shrimp), Faculty of Science, Mahidol University, Rama VI Rd, Bangkok 10400, Thailand. [3]Department of Anatomy, Faculty of Science, Mahidol University, Rama VI Rd, Bangkok 10400, Thailand. [4]Division of Anatomy, School of Medical Science, University of Phayao, Muang, Phayao 56000, Thailand. [5]Aquatic Animal Health Research Team (AQHT), National Center for Genetic Engineering and Biotechnology (BIOTEC), National Science and Technology Development Agency (NSTDA), Yothi office, Rama VI Rd, Bangkok 0400, Thailand.
*These authors contributed equally to this work.

‡Author for correspondence (thanapong.kru@mahidol.edu)

W.P., 0000-0002-5198-4068; A.P., 0000-0003-4198-7748; N.M., 0000-0001-5412-9924; R.V., 0000-0002-8712-7578; T.K., 0000-0003-3191-5564

Received 17 January 2019; Accepted 23 April 2019

INTRODUCTION

The Pacific whiteleg shrimp [*Penaeus* (*Litopenaeus*) *vannamei*] and the giant tiger shrimp (*Penaeus monodon*) (called the black tiger shrimp in Thailand) are the most commonly cultivated shrimp species in Thailand and constitute an important export product (Engle et al., 2017). The shrimp culture industry is continually threatened by emerging diseases caused by pathogens such as viruses, bacteria and protozoa (Thitamadee et al., 2016). Many of these pathogens target vital organs such as those of the alimentary tract. This consists of the mouth, esophagus, stomach (anterior and posterior stomach chambers, ASC and PSC), hepatopancreas (HP, combined functions similar to the liver and pancreas in vertebrates and sometimes called the midgut gland), anterior midgut cecum (AMC), midgut (MG or intestine), hindgut, posterior midgut cecum (PMC) and anus.

In shrimp defense against pathogens, the cuticle (a non-living external layer containing the polymer chitin) is the primary physical barrier. Cuticular structures are hard when calcified but soft and flexible when not. For example, the un-calcified cuticle between abdominal segments (articular elements) is soft to allow flexing, in contrast to the generally hardened, relatively inflexible shell. For the following description of the shrimp alimentary system, we use the terminology of Bell and Lightner (1988). Unlike that of vertebrates, the shrimp stomach is of ectodermal embryonic origin, and so the cuticle from the external body surface is continuous with the inner surface of the esophagus, the stomach and the hindgut near the anus (Meiss and Norman, 1977). When shrimp molt (undergo ecdysis), the cuticle of the outer surface, the mouth, the esophagus, the stomach and the end of the hindgut is sloughed and replaced by a previously generated underlying cuticle. Some parts of the stomach cuticle are soft (un-calcified) while others (e.g. ossicles to grind food) are hardened (calcified). However, similar to the vertebrate intestine, the epithelium of the homologous shrimp MG and its associated organs (i.e. HP, AMC, MG and PMC) are of endodermal origin and their lumens are not covered with cuticle. Thus, there is a transition in the alimentary system from the cuticle-covered stomach to the subsequently uncovered regions up to the end near the anus, where the cuticular covering resumes. At the same time, the epithelial cells of the MG produce a multilayered peritrophic membrane (PTM) that forms a chitinous layer that surrounds the MG contents and has an exclusion diameter of approximately 20 nm (Martin and Hose, 2010).

At the anterior end of the shrimp body, the transition from cuticle to no cuticle takes place at the dorsal, posterior end of the ASC and at the posterior end of the PSC or pyloric (from the Ancient Greek pulōrós or ‘gatekeeper’) region where the gastric sieve (GS) is located. Similar structures are widely reported in crustacean species. After mechanical and chemical digestion in the ASC, relatively large, liquid-borne particles pass from the dorsal end of the ASC directly into the intestine, without passing into the PSC. The PSC is

Journal of Experimental Biology (2019) 222, jeb199638. doi:10.1242/jeb.199638

List of abbreviations

AMC	anterior midgut cecum
ASC	anterior stomach chamber
GS	gastric sieve
HP	hepatopancreas
LAH	lower ampullary half
LSG	longitudinal inter-setal grooves
MG	midgut
PB	phosphate buffer
PBS	phosphate-buffered saline
PMP	posterior median plate
PS	primary setae
PSC	posterior stomach chamber
PSCD	dorsal sub-chamber of the PSC
PSCV	ventral sub-chamber of the PSC
PTM	peritrophic membrane
SEL	size exclusion limit
SEM	scanning electron microscopy
SS	secondary setulae
TP	triangular pyramid
UAH	upper ampullary half

located ventro-medially to the ASC and is separated from it by a relatively narrow, longitudinal slit in the ventro-medial ASC wall that leads first into a dorsal sub-chamber (PSCD) and then via another narrowing into a ventral sub-chamber (PSCV) where the GS is located. Entry to the PSCV is partially obstructed by longitudinal brush-like setae extending up from the dorsal midline of the underlying GS that is an integral part of the PSCV. Together, the narrow slit and the brush-like setae extending from the GS and from the adjacent stomach walls serve as a primary filtration apparatus that allows entry of only liquids and relatively small particles into the PSCV, which serves as a kind of secondary filtration chamber where the GS is located.

Basically, the GS serves as a size-partitioning structure that allows liquids containing dissolved nutrients and very fine particles from masticated and pre-digested stomach contents to enter the HP via right and left hepatopancreatic ducts, where further digestion and transfer of nutrients into the hemolymph takes place. Particles too large to pass through the GC are conducted out of the PSCV through a separate channel to join the coarser material going directly into the intestine from the dorsal region of the ASC.

This process has been described in detail for the river prawn *Macrobrachium carcinus* (Order Decapoda) (Lima et al., 2016) and the mountain shrimp *Anaspides tasmaniae* (Order Syncardia) (Wallis and Macmillan, 1998). Structural and morphological investigation of the GS has also been reported for many decapod species, e.g. *Penaeus* (*Marsupenaeus*) *japonicus* (Lin, 1996), *Pleoticus muelleri* (Díaz et al., 2008), *Nematocarcinus lanceopes*, *Notocrangon antarcticus* and *Chorismus antarcticus* (Muhammad et al., 2012), *P. monodon* and *Metapenaeus ensis* (Lin, 2000) and *M. carcinus* (Lima, et al., 2016). All these studies reported the same pattern of GS organization as an inverted-V, dome-like structure covered with numerous stacks of overlapping fine setae and located at the ventro-medial side of the PSC.

Recently, the pore size (exclusion limit) of the GS in sub-adult *P. monodon* has been determined using various sizes of inert digestibility particles. Particles larger than 3 µm were rapidly excluded while those smaller than 400 nm stayed longer in the digestive tract (Wade et al., 2018), suggesting that the exclusion limit was smaller than approximately 3 µm. In addition, it is widely believed among shrimp pathologists (T. W. Flegel, personal communication) that the GS is normally able to exclude bacteria from the HP because histological and ultrastructural examination of the HP tissue of normal (healthy) shrimp does not reveal the presence of bacteria in the HP lumen even when they are abundant in the stomach and MG of the same specimens, as previously reported (Hopkin and Nott, 1980). Also, when *P. monodon* was challenged with *Vibrio* spp. by immersion and oral intubation, only soluble digested bacterial antigen (i.e. no intact bacteria) could be detected in the HP (Alday-Sanz et al., 2002). In contrast, anal intubation with *Vibrio* spp. has been shown to result in HP tubule infection and disease (Song et al., 1993), suggesting that bacterial introduction with pressure against the internal anatomical structures and mechanics resulted in disruption of the normal exclusion process.

Because of the information summarized above, we hypothesized that the shrimp GS has the capability to exclude particles 1 µm or larger from entering the HP and that this hypothesis could be tested by using polystyrene microspheres and by ultrastructural examination of the GS. Fluorescent polystyrene microsphere tracking has been widely used for many purposes such as determining the size of bacteria and phytoplankton that rotifers consume (Ooms-Wilms et al., 1995; Agasild and Nõges, 2005), tracing the transition in planktonic food webs (Cole et al., 2013), investigating the existing functions and development of the GS in different larval stages of the Eastern spiny lobster *Sagmariasus verreauxi* (Simon et al., 2012) and assisting in biomedical and nanoparticle studies (Jiang et al., 2017).

The aim of our study was to investigate the exclusion limit of the GS in two species of penaeid shrimp (*P. monodon* and *P. vannamei*) using a combination of approaches including inspection of gross morphology, histology and visualization of fed fluorescent microbeads. We also compared the structure of the GS between *P. monodon* and *P. vannamei* to look for possible differences between the species and at different life stages in *P. vannamei*. Our experiments revealed that the GS exclusion limit was less than 1 µm, that the sieve pore diameter was approximately 0.2–0.7 µm, and that there were no significant differences in the GS of *P. monodon* and that of *P. vannamei* or among different developmental stages in *P. vannamei*. The results have ramifications for shrimp nutrition and disease control and provide useful basic knowledge that may also be valuable in the design of novel microfilters for medical and industrial use.

MATERIALS AND METHODS

Animal ethics

All the experiments and procedures used with shrimp in this study were approved by the Faculty of Science, Mahidol University Animal Care and Use Committee SCMU-ACUC, Faculty of Science, Mahidol University, Thailand (no. MUSC61-007-409).

Experimental animals

Broodstock specimens (average body mass 50–60 g) and juveniles (average body mass 5–8 g) of the whiteleg shrimp, *Penaeus vannamei* Boone 1931, and the giant tiger shrimp, *Penaeus monodon* Fabricius 1798, were obtained from local farms in Nakhon Nayok province and Chonburi province, Thailand. They were transported to and maintained in aquaria containing artificial seawater (Marinium, Mariscience Int. Co. Ltd) at 20 ppt and at ambient temperature (27–29°C) with sufficient aeration at Mahidol University, Phayathai campus, Bangkok, Thailand. The shrimp were fed with commercial food pellets (Betagro) twice per day and excess feed was removed twice daily. Shrimp were used for experiments within 7 days of their arrival at the laboratory. Feed was withheld for 3 h prior to experiments.

Journal of Experimental Biology (2019) 222, jeb199638. doi:10.1242/jeb.199638

Tissue preparation

Broodstock shrimp of both species were chosen for gross anatomical and morphological investigations because their GS was significantly larger than that in the smaller shrimp. For gross anatomical and histological investigations of the gastrointestinal tract (including the GS), shrimp were anesthetized and killed following the AVMA Guidelines for the Euthanasia of Animals (Leary et al., 2013). Briefly, shrimp were submerged in ice for 15 min until no movement was observed. Then, the stomach and HP were removed and fixed in 2.5% glutaraldehyde with 4% paraformaldehyde in 0.1 mol l^{-1} phosphate buffer (PB) solution for scanning electron microscopy (SEM), and Davidson's fixative solution for routine histology. For histology, tissues were fixed for 24 h in Davidson's fixative and processed for sectioning and staining with hematoxylin and eosin as previously described (Bell and Lightner, 1988), and they were examined using a light microscope (Leica DM750) with a digital camera (Leica ICC50 HD).

SEM with broodstock and juvenile shrimp

After fixing with 2.5% glutaraldehyde with 4% paraformaldehyde in 0.1 mol l^{-1} PB solution overnight, tissues were washed 3 times (15 min each) with 0.1 mol l^{-1} PB, pH 7.4 at 4°C. They were post-fixed with 1% osmium tetroxide (OsO_4) in 0.1 mol l^{-1} PB at 4°C for 2 h followed by gentle washing 3 times with 0.1 mol l^{-1} PB at 4°C. Next, they were dehydrated through increasing concentrations of ethanol (30%, 50%, 70%, 80%, 90% and 95%), ending with absolute ethanol at 4°C for 15 min (2 times each). The specimens were dried with a critical drying point machine (Hitachi HCP-2) under liquid CO_2 and mounted on stubs with double-coated conductive carbon tape. Finally, they were coated with platinum and palladium in a HitachiE-120 ion sputter device and observed under a Hitachi scanning electron microscope S-2500.

Fluorescent bead preparation and feeding

Commercial food pellets (Betagro) (1 g) were immersed in 100 µl of fluorescent bead solution (either 0.1 or 1 µm diameter, for groups 1 and 2, respectively; see below) (Thermo Fisher Scientific) at a concentration of 1×10^6 beads ml^{-1} in 0.1 mol l^{-1} phosphate-buffered saline (PBS) for 3 h. Control food pellets (group 3) were immersed in PBS only. Thereafter, all were left to dry at room temperature for at least 5 h. Each shrimp was fed with three pellets in separate aquaria.

Determination of feeding time interval

Juvenile shrimp of both species were selected for the feeding experiments using food pellets containing 0.1 µm fluorescent microbeads. After feed administration, translocation of the fluorescent microbeads within individual shrimp was examined using a fluorescence stereomicroscope (Macro Zoom Imaging System MVX10, Olympus) at 4× magnification and at 3, 6, 10 and 100 min post-feeding. Results from different time points were compared with those of shrimp given the control feed with no fluorescent microbeads (group 3).

Determination of the size of the GS

Juvenile shrimp were divided into three groups (3 replicates per group) and fed with commercial food pellets containing either 0.1 or 1 µm fluorescent microbeads (test shrimp groups 1 and 2, respectively) or no microbeads (i.e. normal food pellet control, group 3). Each shrimp was killed on ice 5 min after feeding, then fixed with 4% paraformaldehyde for 24 h. Tissues were immersed in

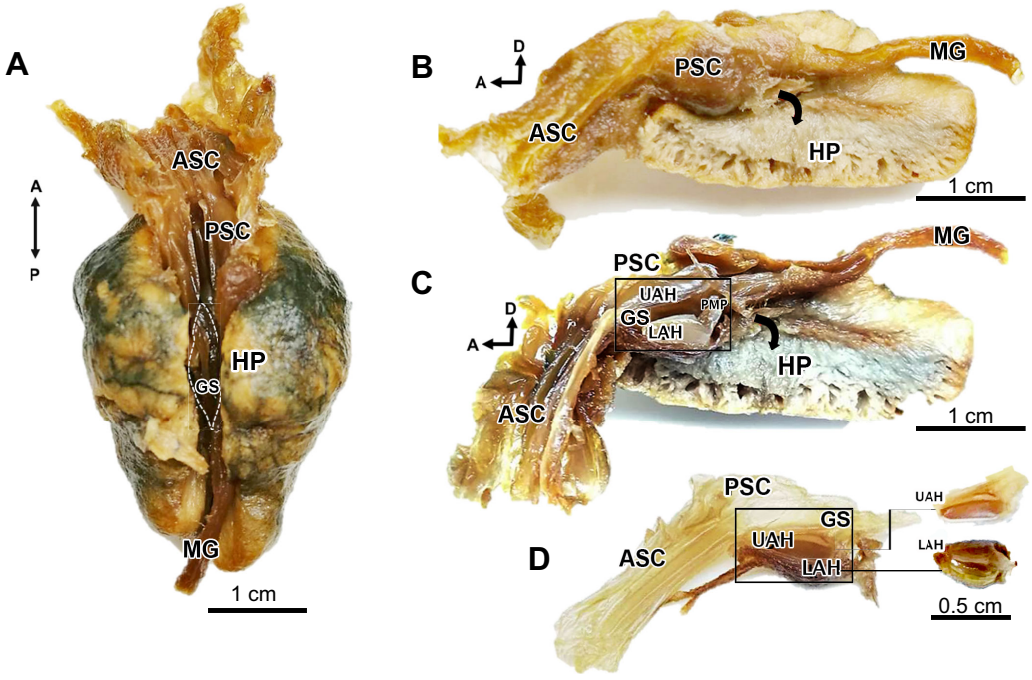

Fig. 1. Gross anatomy of the foregut and its ossified structures in an example penaeid shrimp, *Penaeus monodon*. (A) Photograph of the dorsal view of a dissection of the anterior stomach chamber (ASC) connected to the midgut (MG) and showing the medial–ventral, slit-like opening into the posterior stomach chamber (PSC) consisting of a dorsal sub-chamber (PSCD) and an occluded ventral sub-chamber (PSCV) where the gastric sieve (GS) (indicated by a dashed line) is located at the medial–ventral side. (B) A parasagittal section with the left hemisphere of the hepatopancreas (HP) removed to show the left gastro-hepatopancreatic duct opening from the GS in the PSCV (black arrow). (C) A parasagittal section passing through the internal chamber of the PSC, close to the region of the GS. The walls of the PSCD and PSCV (labeled UAH, upper ampullary half) have been folded back to reveal the outer wall of the GS (labeled LAH, lower ampullary half). PMP, posterior median plate. (D) Dissection of the right wall of the PSCV (labeled UAH) and the GS (labeled LAH). A, anterior; P, posterior; D, dorsal.

Journal of Experimental Biology (2019) 222, jeb199638. doi:10.1242/jeb.199638

sucrose solution of increasing concentration (10%, 20% and 30% for 5 h, 5 h and overnight, respectively) at 4°C. Once the tissue was confirmed to sink, it was embedded in OCT compound and cut with a cryostat microtome (Leica) to 7 µm thickness. Each tissue sample was examined under a fluorescence microscope BX53 (Olympus). Additional shrimp were similarly fed, anesthetized and prepared for observation by SEM as described above.

RESULTS

Gross anatomy of the penaeid shrimp stomach

The gross anatomy and histology of the stomach structures in penaeid shrimp are shown in Fig. 1, using a specimen of *P. monodon* as an example. In Fig. 1A, the ASC has been opened to expose the slit-like portal leading into the PSC, most of which is overlaid by the HP tissue in this image. The PSC consists of a dorsal sub-chamber (PSCD) and a ventral sub-chamber (PSCV) that cannot be seen in Fig. 1A but contains the GS, the position of which is shown with a dashed outline. In Fig. 1B, a lateral view with half of the HP removed shows the whole PSC and its relationship to the ASC. During eating, liquid containing large particles passes from the dorsal side of the ASC directly into the MG, which is homologous to the vertebrate intestine. Liquid with dissolved nutrients and smaller particles passes into the PSCD and then into the PSCV where the GS is located. The GS selectively filters liquids containing nutrients and sub-micrometer particles (see later) that are shunted ventrally into the HP via hepatopancreatic ducts, the left one of which is indicated in Fig. 1B. Particles that cannot pass through the filter are shunted dorsally into the MG to join material coming directly from the AMC and destined for excretion. In Fig. 1C, the PSC has been cut open and the PSCD and PSCV walls have been folded back to reveal the GS that is an integral part of the base of the PSCV. A spearhead-like structure called the posterior median plate (PMP) is situated at the posterior end of the GS, serving as the route for material excluded by the filter that is shunted dorsally into the MG. These structures are shown at higher magnification in Fig. 1D.

Histology of the PSC using freezing-microtome and semi-thin sections

Fig. 2A shows a photomicrograph of a frozen tissue cross-section of the cephalothorax through the PSC, surrounded by HP tissue. It reveals the relationship between the dorsal chamber (PSCD) and ventral chamber (PSCV), the latter containing the GS with the closely adjacent PSCV wall. The enlargement in Fig. 2B clearly reveals that both the chamber wall (labeled upper ampullary half, UAH) and the GS (labeled lower ampullary half, LAH) are covered with a carpet of setae. It also clearly shows the longitudinal inter-setal grooves (LSG) that underlie the setal layers. Note also that the dorsal, midline crest of the GS has an extension that is spike like in cross-section with a smooth base and short stalk that then expands into a brush-like head. In Fig. 2C, a similar section through the PSC of a different specimen shows a nascent, replacement GS forming below the existing one (i.e. in preparation for the next molt).

In addition to frozen tissue sections, some specimens were embedded in epoxy resin for preparation of semi-thin sections (Fig. 3) that gave more detailed images of the PSCV structure. In Fig. 3A, the central spike of the GS crest can be seen to extend into the slit between the PSCD and PSCV, together with its covering of setal extensions and with other long setae on either side that arise directly from the top of the GS on either side of the midline. The adjacent PSCV wall or UAH is also covered with long setae. An enlarged image of the LSG (Fig. 3B) shows that they lie at the base of the overlapping ranks of setae on the GS surface (labeled LAH). The higher magnification in Fig. 3B shows that all the setae have sub-branches (setulae) that extend at an outward, dorso-lateral angle with respect to the surface of the GS. The particles found within the LSG are sub-micrometer in diameter.

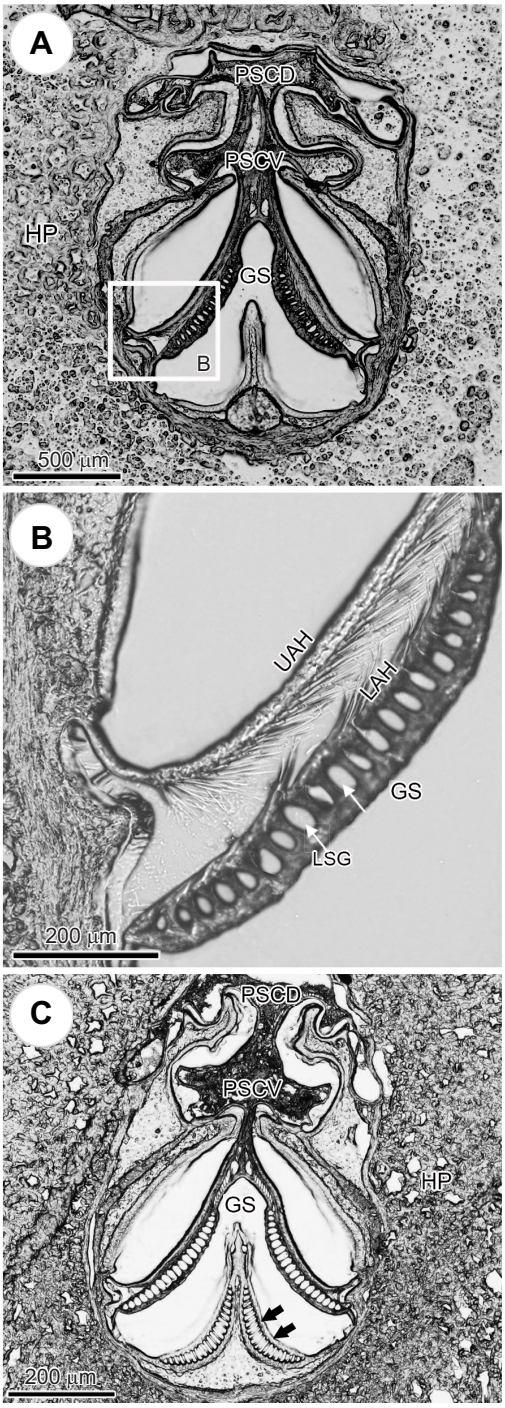

Fig. 2. Photomicrographs of frozen tissue sections of the shrimp cephalothorax in the region of the PSC. (A) Low magnification image showing the PSCD and PSCV. Note the narrow passage between the PSCD and PSCV and that the crest at the midline of the GS extends upward from the GS and inserts into the passage. (B) High magnification image of the boxed region in A, showing that the surface of the PSCV (labeled UAH) and the adjacent GS (labeled LAH) are both covered with setae. (C) Low magnification image similar to that in A but from a different shrimp specimen and showing a nascent GS (black arrows) present below the currently operating GS (i.e. in preparation for the next molt).

Journal of Experimental Biology (2019) 222, jeb199638. doi:10.1242/jeb.199638

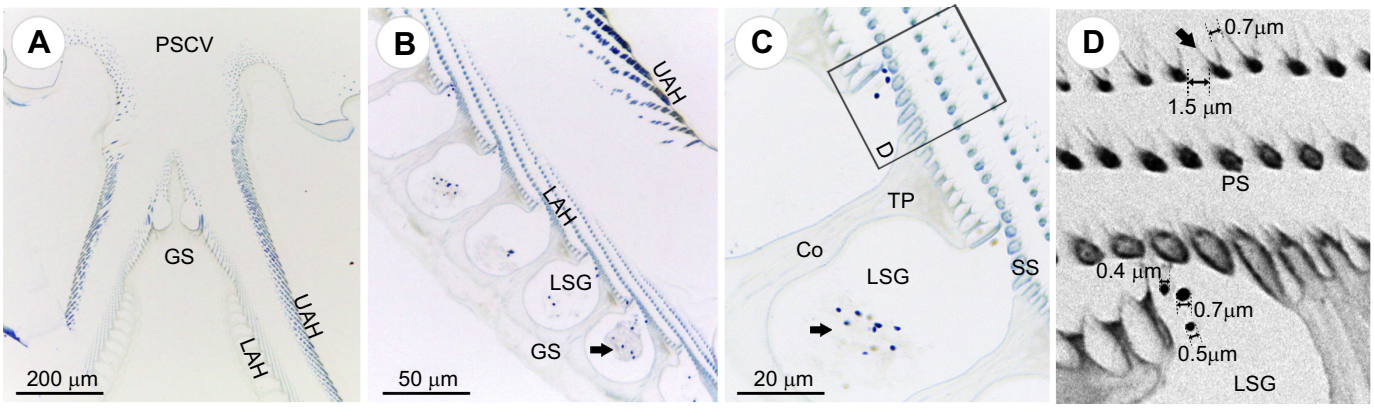

Fig. 3. Photomicrographs of transverse, semi-thin sections through the GS stained with Toluidine Blue. (A) Low magnification image of the GS showing the PSCV wall (labeled UAH) and the GS (labeled LAH). (B) Medium and (C) high magnification of the GS showing small food particles in the LSG (arrow). Co, core. (D) Magnification of the boxed region in C, showing the diameter of food particles in an LSG (0.2–0.7 µm). The width of the space between the primary setae (PS) is approximately 1.5–1.7 µm, while that between the secondary setulae (SS, arrow) is approximately 0.5–0.7 µm.

SEM of the GS

SEM photomicrographs of the morphology of GS structures are shown in Fig. 4 for juvenile *P. vannamei* (Fig. 4A–I) and broodstock *P. monodon* (Fig. 4J–O). In Fig. 4A, the PSC of *P. vannamei* has been cut open and the setae-covered walls of the dorsal (PSCD) and ventral (PSCV) chambers have been folded back to reveal the underlying GS as an elongated, inverted-V-like dome arising medially from the bottom of the PSCV at its posterior end. In Fig. 4B, the carpet-like, overlapping layers of setae on the GS surface can be seen and are progressively enlarged in Fig. 4C–E to clearly reveal the dorso-lateral branches (setulae) that were seen near the limit of light microscope resolution in the semi-thin sections in Fig. 3C. The space between these secondary setulae was approximately 0.2–0.7 µm (Fig. 3D).

In Fig. 4F, the rows of setae along the midline crest of the GS (cf. Fig. 3A by light microscopy) can be seen from the left side only, with the matching structures on the right side of the GS in shadow. They consist of two distinctive types. Both have secondary setulae, but one setal type has hooked ends (Fig. 4H) and the other not. In reference to Fig. 3A, the hooked setae (Fig. 4H) arise directly from the upper surface of the GS on either side of the midline, while the non-hooked ones (Fig. 4G) arise from the enlarged end of the smooth extension from the GS midline. At the posterior end of the GS, there is a spearhead-shaped PMP (Fig. 4I) with long setae, presumed to direct the flow of GS-excluded particles into the MG (see above). Similar structures to these were seen in SEM photomicrographs of *P. monodon* (i.e. branching setae covering the GS in Fig. 4K–N and a PMP in Fig. 4J). One difference from *P. vannamei* was that the tips of the primary setae in *P. monodon* were not straight but looped back and enmeshed in the setal mat.

Details of the LSG by SEM (Fig. 4M–O) are shown for *P. monodon* only, but they are similar in *P. vannamei*. In Fig. 4M, the GS was cut open to reveal the LSG and the overlying layers of setae, portions of which are enlarged in Fig. 4N and O. These images can be compared with the photomicrographs from frozen tissue sections (Fig. 2) and semi-thin sections (Fig. 3). The transverse section of the GS passing through the mid-part shows overlapping rows of primary setae aligned to form the surface of the GS (Fig. 4M,N). They arise from single triangular heads (triangular pyramid, TP; Fig. 4O) attached to the 'setal core' (Co; Fig. 4O) that consists of fused setae, together forming the dorsal wall of one LSG and the ventral wall of another (Fig. 4N, see also the semi-thin sections in Fig. 3B,C). The TP is also lined with setulae along its length, similar to the elongated setal arms that extend from the TP (Fig. 4O).

From all of the information above, we propose a model for food transportation through the GS, as illustrated in Fig. 5. The arrangement and stacking of the primary setae (PS) and its secondary setulae (SS) show that the gaps between the PS and SS are approximately 1.5–1.9 µm and 0.2–0.7 µm, respectively. The green sphere represents a food particle capable of passing through the PS and SS gaps to collect in the LSG and move in a posterior direction towards the HP.

Detection of fluorescent bead translocation into the gastrointestinal tract

Microbead fluorescence could be observed through the translucent tissue from the mouth to the anus (Fig. 6). The signal could be seen in the ASC and PSC 3, 6 and 10 min after feeding (Fig. 6A–C). The signal was also visible in the surrounding areas from 6 min (Fig. 6B, arrow) to 10 min (Fig. 6C), indicating that the microbeads had also moved into the HP. Fluorescence was initially detected in the area of the MG at 6 min (Fig. 6B) and strongly detected at 10 min (Fig. 6C, arrow). By 100 min after feeding, fluorescence had decreased in the ASC, PSC and HP, and was most prominent in the MG and HG regions (Fig. 6D, arrows). The control group fed with normal food pellets did not show any fluorescence in the gastrointestinal tract (Fig. 6E).

Sieve size determination using fluorescent microbeads

After shrimp were fed for 5 min with the 0.1 µm fluorescent microbeads, a fluorescence signal was found in the dorsal and ventral chambers of the PSC (Fig. 7A,B). At higher magnification, fluorescence was detected in the PSCV in the narrow space between the setae-covered wall of the PSCV and the GS surface (Fig. 7B′) and also in a hepatopancreatic duct (Fig. 7C). Fluorescence was also seen in HP tubule lumens (Fig. 7D,F,G) and within the cytoplasm of HP tubule epithelial cells (Fig. 7E).

By contrast, fluorescence from the 1 µm microbeads was found only in the PSCD lumen and in the PSCV luminal space between the stomach wall and GS surface (Fig. 8A,B). No fluorescence was seen in the LSG, in the HP tubule lumens or in the cytoplasm of HP tubule epithelial cells (Fig. 8C,D). Nor was there any microbead fluorescence in the HP, either in the tubule lumens or in the tubule

Journal of Experimental Biology (2019) 222, jeb199638. doi:10.1242/jeb.199638

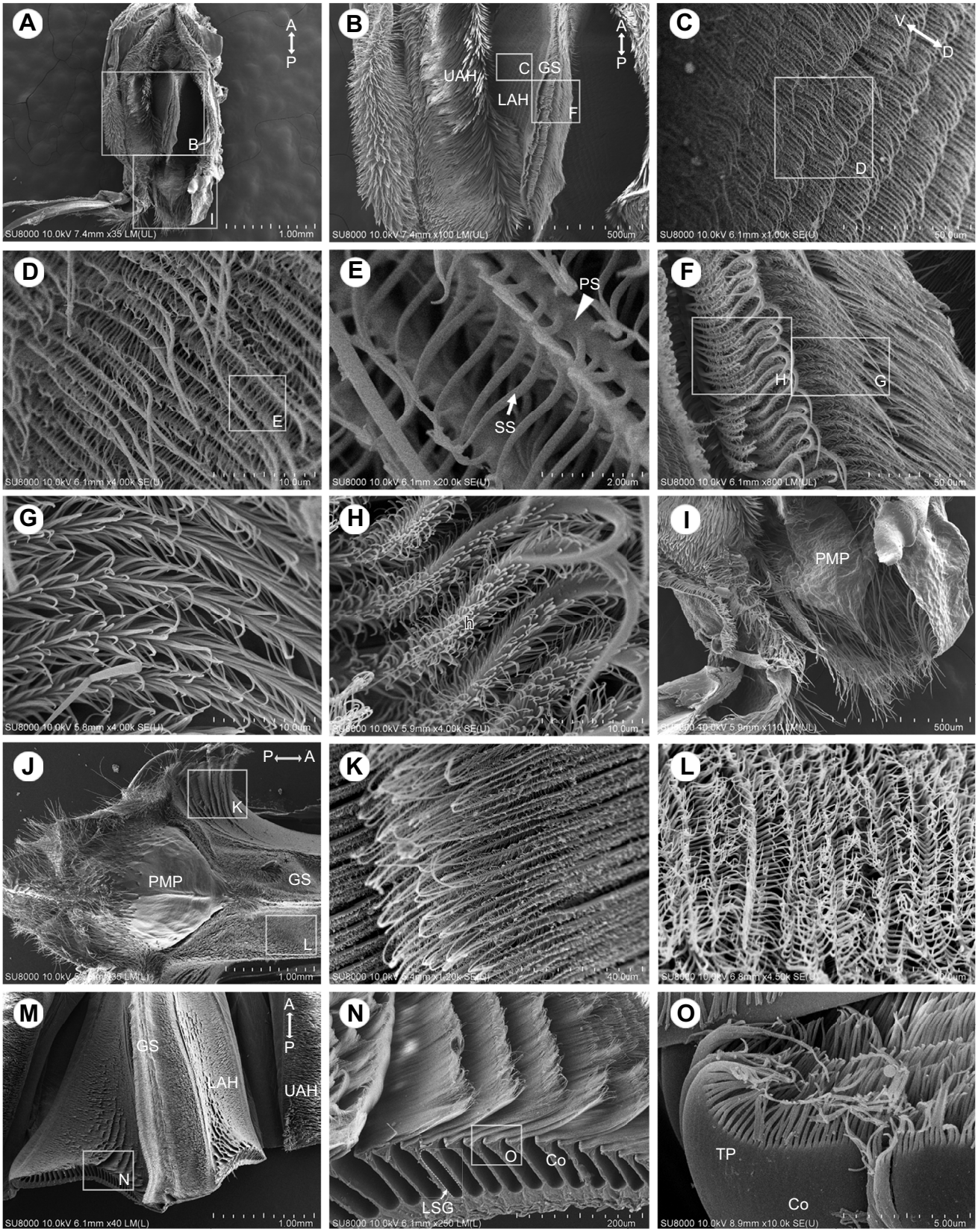

Fig. 4. See next page for legend.

epithelial cells (Fig. 8E,F). The control shrimp fed with normal pellets showed a degree of autofluorescence from the feed in the PSCV (Fig. 8G), but none in the LSG or HP (Fig. 8H,I).

Conclusions

The GS of penaeid shrimp is located at the base of the PSC and is connected to the HP via posterio-lateral gastro-hepatopancreatic ducts.

Journal of Experimental Biology (2019) 222, jeb199638. doi:10.1242/jeb.199638

Fig. 4. Scanning electron micrographs of morphological features of the GS in juvenile penaeid shrimps. (A–I) Juvenile *P. vannamei* and (J–O) broodstock *P. monodon*. (A) Top-view of PSC with the lateral walls of the PSCD and PSCV (labeled UAH) folded back to show the GS (B) (labeled LAH). (C) A low magnification view showing the overlapping, comb-like rows of primary setae (PS) covering the surface of the GS. (D,E) Progressively higher magnifications of the boxed region in C (and D), showing secondary setulae (SS) branching from each of the PS. (F) Medium magnification of two distinctive types of setae found along the dorso-medial crest of the GS. (G,H) Higher magnification of setae type I (hooked, h) and type II, respectively, that also carry branching setulae. (I) View of the posterio-median plate (PMP) with long setae at the posterior end of the GS. (J) PMP at the posterior end of the GS of *P. monodon*. (K) Medium magnification of the surface of the GS of *P. monodon* showing overlapping combs of setae. Note that the ends of the setae are looped back to intermesh with the setal mat. (L) Higher magnification of K, showing the laterally branching setulae on the setae. (M) Transverse section of the GS showing an end-on view of the longitudinal setal grooves (LGS) at the bases of the setal combs. (N,O) Progressively higher magnifications of the boxed region in M (and N), showing the setal core (Co) and triangular pyramid (TP). A, anterior; P, posterior; V, ventral; D, dorsal.

The GS is a non-living, V-shaped, dome-like, cuticular structure covered with comb-like rows of setae with dorso-lateral branches that arise at an approximate right-angle from fused setae that form the walls of the LSG of the GS. Food particles larger than 1 µm cannot pass through the setal layers into the LSG and are instead transported directly to the MG via the PMP. In contrast, food particles substantially smaller than 1 µm move down through the setal matt and enter the LSG to be transported to the HP via the hepatopancreatic ducts (Fig. 5).

DISCUSSION

Our results for the structure of the penaeid shrimp ASC, PSC and GS are similar to those previously reported for *P. japonicus* (Lin, 1996) and for other crustacean species, including the spider crab, *Notomithrax ursus* (Woods, 1995), the Brazilian native prawn, *M. carcinus* (Lima et al., 2016) and three Antarctic shrimp species (*N. lanceopes*, *N. antarcticus* and *C. antarcticus*) (Storch et al., 2001). Most of these reports focused mainly on the relationship between the structure and dietary habits of each species. However, the overall GS structure in these various decapods was very similar even though their diets differed, as observed earlier for three species of southern African decapods (Schaefer, 1970).

Despite these earlier reports, little work has been done on the size exclusion limit (SEL) for GS conservation over the life span of crustaceans, particularly the important aquatic penaeid species, i.e. *P. vannamei*. For example, the width of setae covering the GS was proposed to be approximately 1 µm in adult *P. japonicus* (Lin, 1996). Recently, the investigation of Wade et al. (2018) reported that the GS in sub-adult *P. monodon* allowed particles below 400 nm to pass through into the HP lobules. However, larger molecules (>3 µm) were excluded by the GS and consequently excreted within 1 h. Also, the pore size of the GS of the spiny lobster (*S. verreauxi*) was found to be smaller than 1 µm (Simon et al., 2012). These pieces of evidence support our finding that the pore size of GS in two penaeid shrimps was consistent within and even across the species. Here, our results using SEM and fluorescent microbeads support our hypothesis that the SEL of the GS of both species is substantially less than 1 µm, which may explain why whole bacterial cells are rarely present in the lumen of hepatopancreatic tubules in healthy shrimp. This finding has important implications for preparation of shrimp feeds that contain microencapsulated nutritional additives such as vitamins, which have to escape the digestive process in the stomach and enter the HP as quickly as possible. Our results suggest that the size of

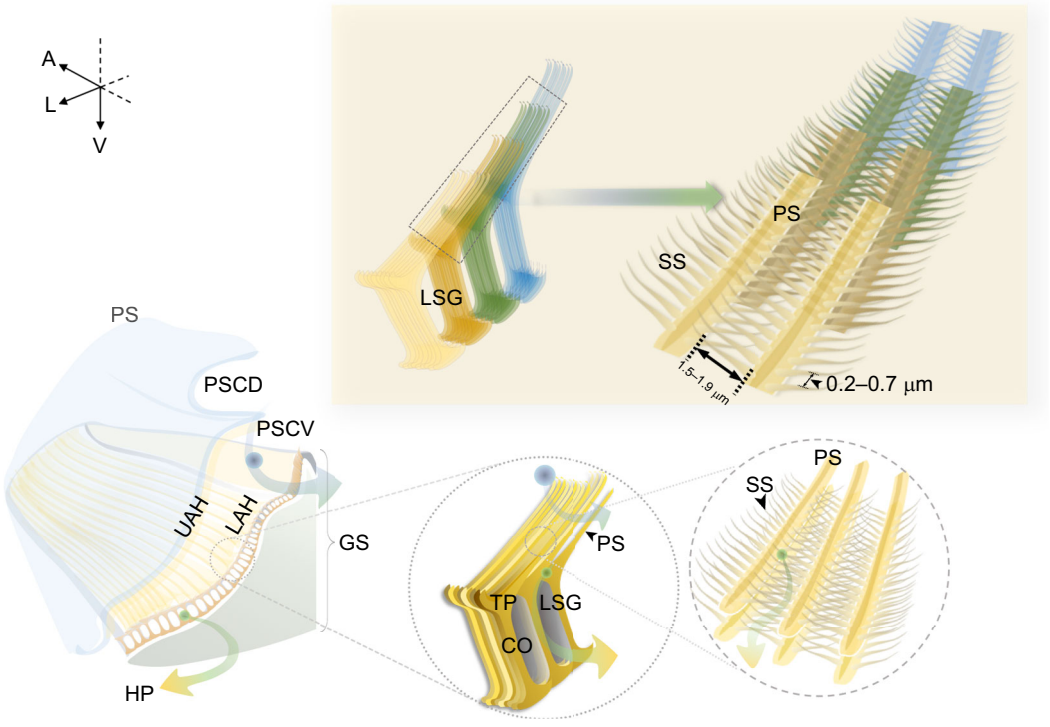

Fig. 5. Schematic illustration showing the size exclusion limit (SEL) and filtering capability of the GS. The arrangement of the stacked setae revealed that the gaps between the PS and SS are approximately 1.5–1.9 µm and 0.2–0.7 µm, respectively. A particle less than 1 µm diameter size (green dot) is able to pass through the SS slots, roll along the PS and move into the LSG. Particles are carried continuously in a posterior direction along the LSG. Finally, they are carried into the HP's lumen via the gastro-hepatopancreatic ducts. In contrast, particles greater than 1 µm diameter (blue dot) cannot pass through the sieve and are carried into the MG. A, anterior; L, lateral; V, ventral.

Journal of Experimental Biology (2019) 222, jeb199638. doi:10.1242/jeb.199638

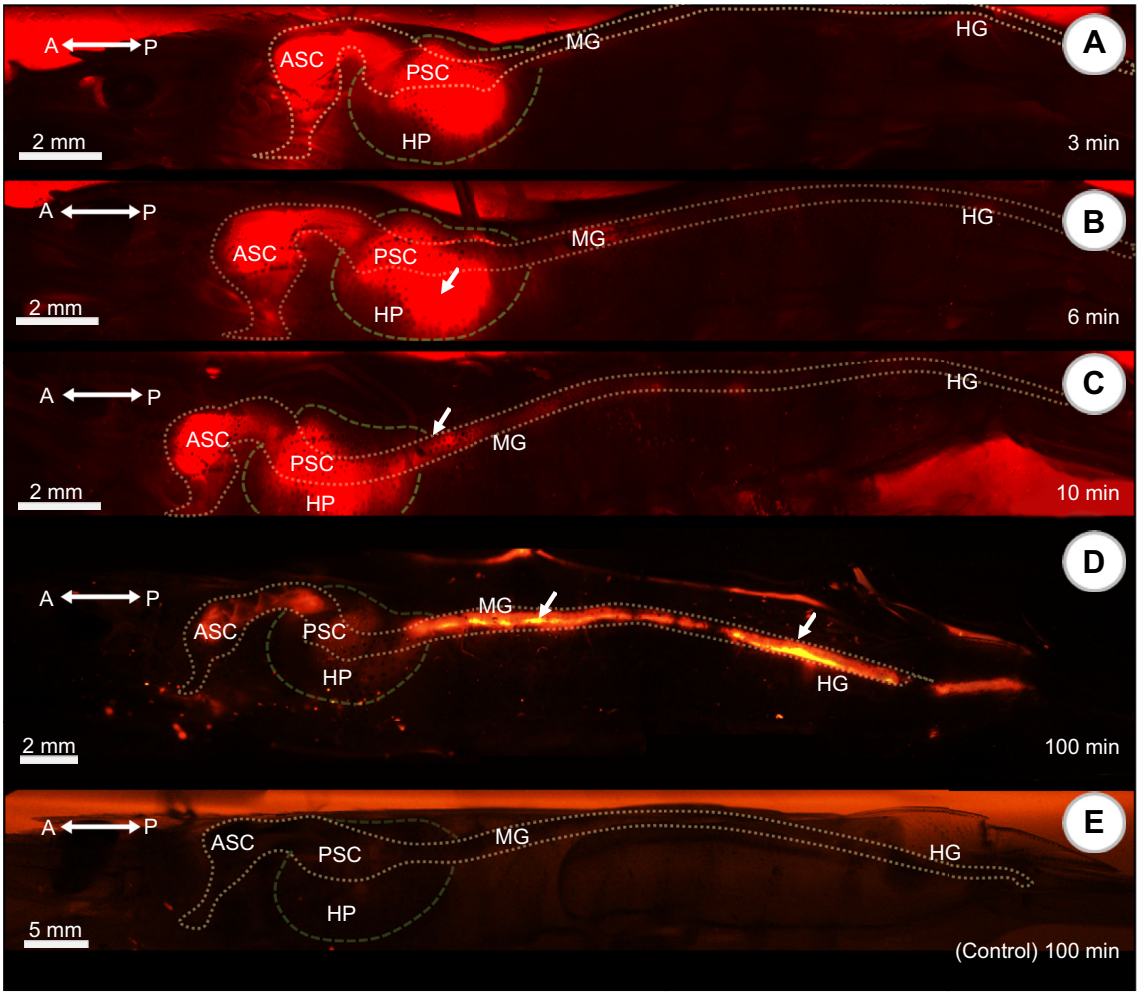

Fig. 6. Detection of the 0.1 µm fluorescent microbead signal along the gastrointestinal tract at different times after feeding. Fluorescence at (A) 3 min, (B) 6 min (signal found in HP, arrow), (C) 10 min (signal found in MG, arrow) and (D) 100 min [signals in hindgut (HG), arrow]. (E) Control group fed with normal food pellets at 100 min. A, anterior; P, posterior.

these particles should be substantially under 1 µm or that they should be designed to enter the PSCV and disintegrate there to enter the HP. Otherwise, larger feed particles would have to be reduced to an appropriate size by the stomach or risk being directed to the MG.

A previous study (Simon et al., 2012) reported that the SEL of the GS of different larval development stages (well developed at stages 3–4) and of juvenile lobster, *S. verreauxi*, remains morphologically unchanged, meaning that once the GS is fully formed, it has a constant filtering capability in healthy shrimp. Interestingly, Gophen and Geller (1984) also found that, by using spherical plastic beads with bacteria, the SEL of the GS of the crustacean *Daphnia* spp. was determined to be approximately 0.4–0.7 µm diameter. This supports our hypothesis that the GS can exclude whole bacteria from the HP.

In the digestive mechanism of crustaceans, movement of the stomach chambers is controlled by a nerve plexus for muscles that allow squeezing, cutting and grinding. The resulting small amplitude pulsating movement in the PSC results in a ‘pumping’ movement that propels food into the MG (McGaw and Curtis, 2013). The muscle attached to the external lateral wall of the PSC is a key modulator of the GS filtering function. Relaxation and contraction of this muscle result in fine particles and liquids moving into the space between the setae-covered surfaces of the PSCV wall and GS. When the two surfaces are pressed together, liquids and particles passing through are squeezed through the setal mat into the LSG (Schaefer, 1970). The action is facilitated by the flexible cuticle lining of the PSCV and its muscle control, but the precise mechanism remains unclear. For example, our frozen cross-sections of the GS of *P. monodon* and *P. vannamei* show relatively large spaces behind the chitinous wall of the PVSC and under the layer of LSG in the GS. Bell and Lightner (1988), in reference to their photomicrograph of the PSCV, describe the space below the LGS as a preparation artifact. However, our frozen tissue sections suggest instead that these spaces are real. This contention is supported by Fig. 2C, where the active GS is separated by such a space from a replacement GS that has formed in preparation for the next molt. Thus, we hypothesize that these spaces are filled with gas and play an important role in the mechanical ‘pumping’ action necessary for the filtering function of the GS. Moreover, it is clear that the chitin-based structure of the GS is a complex, non-living cuticular structure and that its mechanical function does not require attachment to a living layer of underlying epidermal cells. The mechanics of the GS could inspire the construction of a novel sub-micrometer filter that can resist plugging.

The appropriate timing of food passage in juvenile shrimp from the mouth to the anus and the retention of digested food particles in the stomach and alimentary tract are essential for nutrient

Journal of Experimental Biology (2019) 222, jeb199638. doi:10.1242/jeb.199638

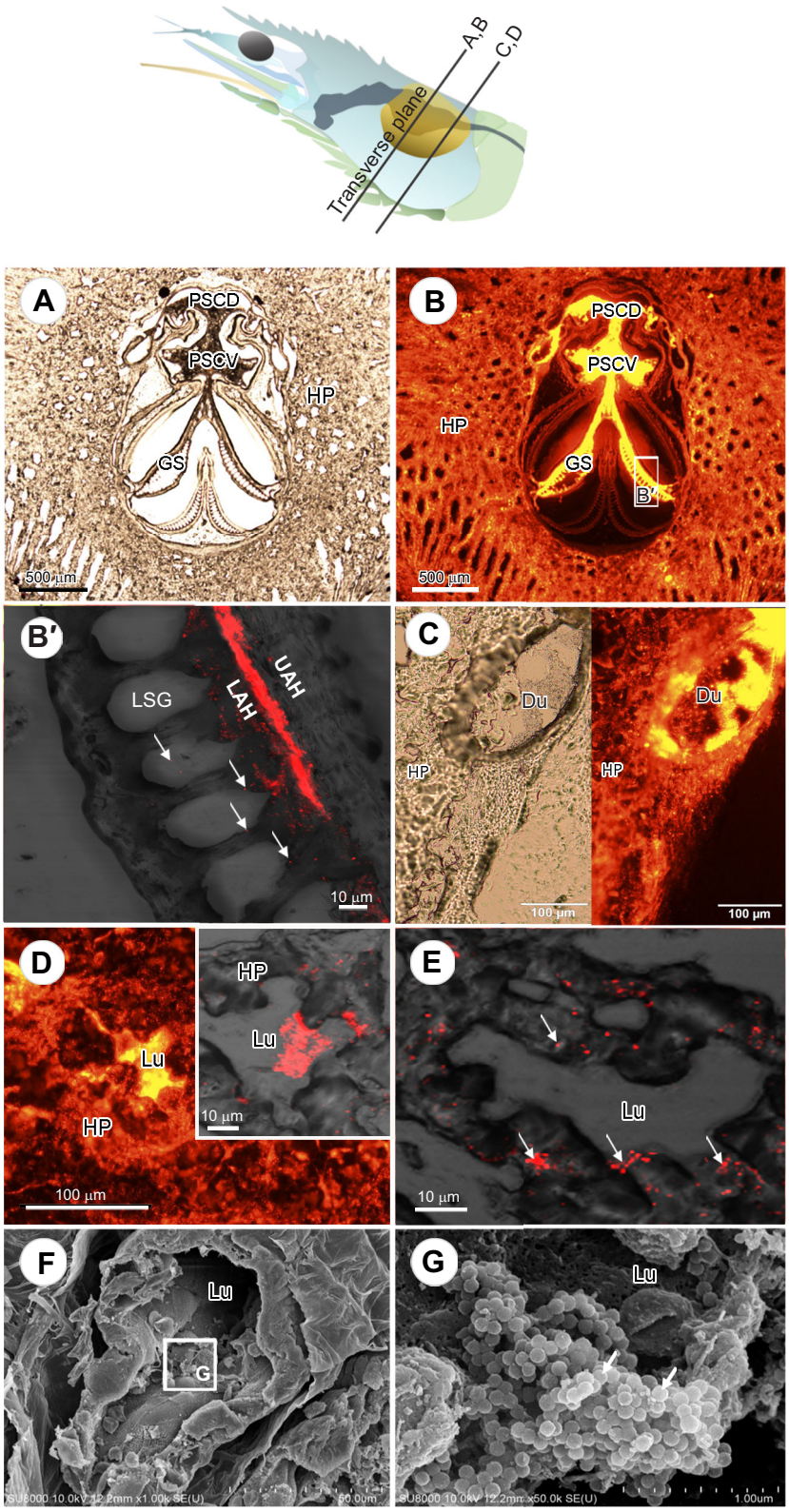

Fig. 7. Transverse sections through the GS region of a shrimp specimen fed with 0.1 µm fluorescent microbeads. (A,B) Fluorescence detected in the PSC, and (B′) the space between the GS surface (labeled LAH) and the PSCV wall (labeled UAH) (boxed region in B), showing microbeads (arrows) passing though the LSG. (C) Fluorescence signal detected in the hepatopancreatic duct (Du) and (D) the HP lumen. (E) The fluorescence detected inside HP tubule epithelial cells (arrows). (F,G) View of 0.1 µm microfluorescent beads (arrows) in the HP lumen by scanning electronmicroscopy.

absorption with maximum efficiency. However, the transit time varies among Decapod species, and might be influenced by the size and type of consumed food, the size and activity of an animal, and any number of other environmental factors including salinity and temperature. A slow transit rate allows more time for nutrient absorption (McGaw and Curtis, 2013). In the adult shore crab, *Carcinus maenas*, the microbeads were retained for up to 2–3 weeks (Watts et al., 2014). However, our study found that the fluorescence in the HP rose and then fell by 100 min after feeding, suggesting that the microbeads ingested by the HP tubule epithelial cells of juvenile shrimp were very much reduced in signal. This is consistent with gut passage times of 1–2 h for other

Journal of Experimental Biology (2019) 222, jeb199638. doi:10.1242/jeb.199638

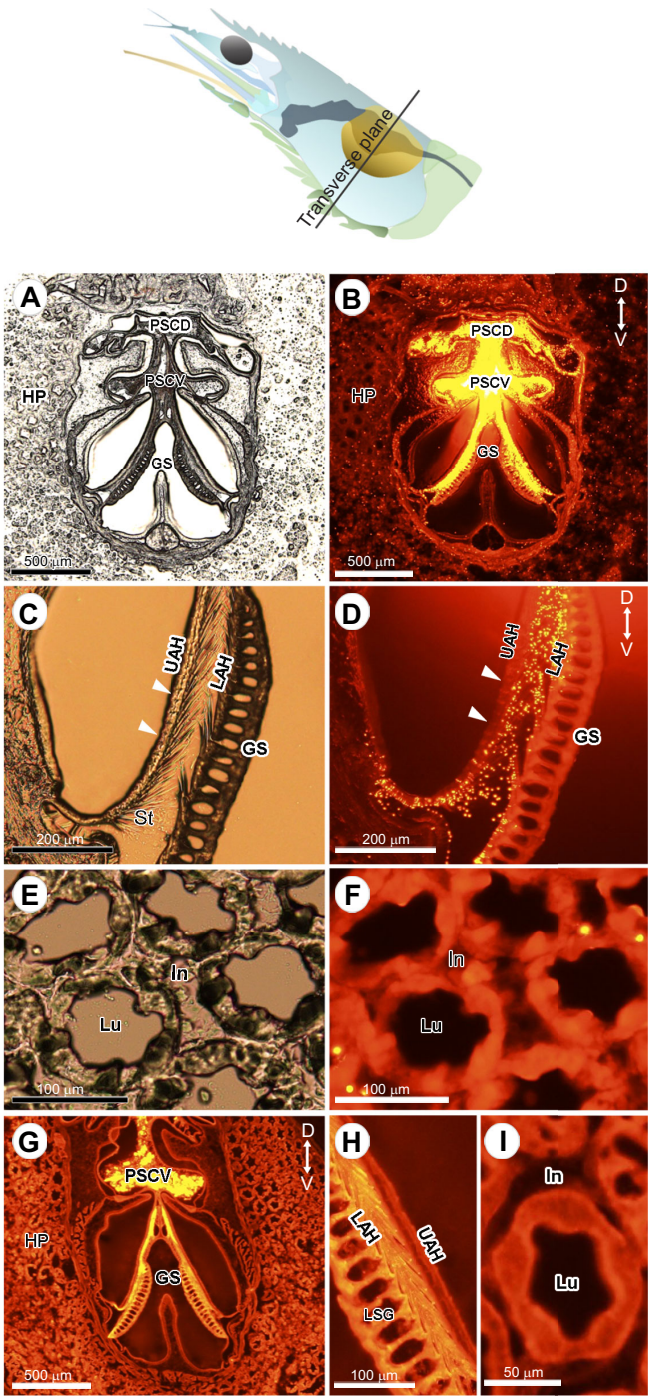

Fig. 8. Transverse section through the GS of a shrimp fed with 1 µm fluorescent microbeads. (A,B) Localization of fluorescence signals in the PSCD and PSCV. (C,D) Fluorescent beads (arrowheads) distributed along the setae in the space between the PSCV wall (labeled UAH) and the GS wall (labeled LAH). (E,F) Absence of fluorescent beads in the HP lumen. (G–I) Histological section of shrimp fed with normal food pellets (negative control) showing no fluorescence in the space between the PSCV wall (labeled UAH) and the GS wall (labeled LAH), in the HP lumen (H) or in HP tubule epithelial cells (I). In, interstitial space. D, dorsal; V, ventral.

penaeid shrimp species (Beseres et al., 2005; Pollack et al., 2006). For sub-adult *P. monodon*, the signal of particles (≤100 µm) in the digestive tract emerged within 1 h and was cleared within 5 h (Wade et al., 2018). Aside from being expelled in feces, there are other possible reasons for the loss of fluorescence from the HP, especially from the cytoplasm of tubule epithelial cells. One is possible translocation from HP cells to the hemolymph and then to other parts of the body such as the ovaries and gills, as reported in *C. maenas* (Farrell and Nelson, 2013; Watts et al., 2014). Alternatively, they might be fragmented into even smaller micro- or nano-particles as reported for millimeter diameter microplastic beads in Antarctic krill (Dawson et al., 2018). It is also possible that engulfed particles may end up in feces after ejection from the engulfing cells or from sloughing of those cells, as has been reported for B-cells that accumulate indigestible materials in vacuoles before they slough into the tubule lumen, to be replaced by new epithelial cells arising in the E-cell region of the HP (Hopkin and Nott, 1980). This is consistent with the report that 0.1 µm microspheres fed to larval lobster were discarded approximately 18–24 h after feeding, during B-cell extrusion. Similarly, B-cells were found to be released after 18 h in juvenile lobster (Simon, 2009). However, there was a small detectable signal in the ASC, PSC and HP at 100 min after feeding, suggesting that at least some of the microbeads might have been trapped inside these complex structures for longer periods of time. Such a long duration of particle retention agrees with a previous finding that small indigestible particles that migrated through into the digestive gland could stay there for up to 24 h (Wade et al., 2018).

In conclusion, understanding the morphology, organization and SEL of the GS in penaeid shrimps has twofold benefits. Firstly, it indicates the involvement of the GS in preventing potentially pathogenic bacteria from entering the HP. However, some bacteria in the stomach can produce toxins that are capable of passing through an intact GS to damage or destroy viral organs (Lightner, 1988; Aguirre-Guzmán et al., 2004). A good current example is acute hepatopancreatic necrosis disease caused by isolates of *Vibrio* species that colonize the shrimp stomach, where they produce Pir-like toxins that pass through the GS and damage HP tubule epithelial cells (Thitamadee et al., 2016). Alternatively, bacteria in the stomach may produce hydrolytic enzymes (Tzuc et al., 2014) that may compromise the GS filtering capacity, facilitating entry of foreign materials into the HP. Secondly, knowledge that the GS is a sub-micrometer filter means that it may serve as a selective route for the introduction of nano-carriers into the shrimp HP and hemolymph for various purposes, ranging from nutrition to disease prevention and control.

Acknowledgements

We extend our gratitude to Dr Kallaya Sritunyalucksana-Dangtip, Dr Charoonroj Chotwiwatthanakun, Dr Jirawat Saetan and Dr Tatpong Tulyananda for their kindness and help. We would also like to thank Prof. T. W. Flegel (National Center for Genetic Engineering and Biotechnology - BIOTEC, National Science and Technology Development Agency - NSTDA) for assistance in preparing and editing the manuscript. Finally, we also thank the reviewers and editor for providing valuable comments and suggestions that improved the manuscript.

Competing interests

The authors declare no competing or financial interests.

Author contributions

Conceptualization: R.V., S.T., T.K.; Methodology: W.P., A.P., N.M., S.T., T.K.; Validation: W.P., T.K.; Formal analysis: T.K.; Investigation: W.P., A.P., N.M., S.T., T.K.; Resources: W.P., N.M., R.V., S.T.; Data curation: W.P., A.P., R.V., T.K.; Writing - original draft: W.P., T.C., S.T., T.K.; Writing - review & editing: T.K.; Visualization: W.P., A.P., R.V., T.K.; Supervision: R.V., S.T., T.K.; Project administration: R.V., S.T., T.K.; Funding acquisition: R.V., S.T.

Funding

This research was supported by a Thailand Research Fund (TRF) research grant (IRG5980001) to S.T. and Mahidol University grant (no. 517832 and 254639) to S.T.

References

Agasild, H. and Nõges, T. (2005). Cladoceran and rotifer grazing on bacteria and phytoplankton in two shallow eutrophic lakes: in situ measurement with fluorescent microspheres. *J. Plankton. Res.* **27**, 1155-1174. doi:10.1093/plankt/fbi080

Aguirre-Guzmán, G., Ruíz, H. M. and Ascencio, F. (2004). A review of extracellular virulence product of Vibrio species important in diseases of cultivated shrimp. *Aquacult. Res.* **35**, 1395-1404. doi:10.1111/j.1365-2109.2004.01165.x

Alday-Sanz, V., Roque, A. and Turnbull, J. F. (2002). Clearing mechanisms of *Vibrio vulnificus* biotype I in the black tiger shrimp *Penaeus monodon*. *Dis. Aquat. Org.* **48**, 91-99. doi:10.3354/dao048091

Bell, T. A. and Lightner, D. V. (1988). *A Handbook of Normal Penaeid Shrimp*. Baton Rouge, LA: World Aquaculture Society, c1988.

Beseres, J. J., Lawrence, A. L. and Feller, R. J. (2005). Variation in fiber, protein, and lipid content of shrimp feed-effects on gut passage times measured in the field. *J. Shellfish. Res.* **24**, 301-309. doi:10.2983/0730-8000(2005)24[301:VIFPAL]2.0.CO;2

Cole, M., Lindeque, P., Fileman, E., Halsband, C., Goodhead, R., Moger, J. and Galloway, T. S. (2013). Microplastic ingestion by zooplankton. *Environ. Sci. Technol.* **47**, 6646-6655. doi:10.1021/es400663f

Dawson, A. L., Kawaguchi, S., King, C. K., Townsend, K. A., King, R., Huston, W. M. and Bengtson Nash, S. M. (2018). Turning microplastics into nanoplastics through digestive fragmentation by Antarctic krill. *Nat. Commun.* **9**, 1001. doi:10.1038/s41467-018-03465-9

Díaz, A. C., Fernández Gimenez, A. V., Velurtas, S. M. and Fenucci, J. L. (2008). Ontogenetic changes in the digestive system of *Pleoticus muelleri* (Decapoda, Penaeoidea). *Invertebr. Reprod. Dev.* **52**, 1-12. doi:10.1080/07924259.2008.9652266

Engle, C. R., McNevin, A., Racine, P., Boyd, C. E., Paungkaew, D., Viriyatum, R., Tinh, H. Q. and Minh, H. N. (2017). Economics of sustainable intensification of aquaculture: evidence from shrimp farms in Vietnam and Thailand. *J. World. Aquacult. Soc.* **48**, 227-239. doi:10.1111/jwas.12423

Farrell, P. and Nelson, K. (2013). Trophic level transfer of microplastic: *Mytilus edulis* (L.) to *Carcinus maenas* (L.). *Environ. Pollut.* **177**, 1-3. doi:10.1016/j.envpol.2013.01.046

Gophen, M. and Geller, W. (1984). Filter mesh size and food particle uptake by Daphnia. *Oecologia* **64**, 408-412. doi:10.1007/BF00379140

Hopkin, S. P. and Nott, J. A. (1980). Studies on the digestive cycle of the shore crab *Carcinus maenas* (L.) with special reference to the B-cells in the hepatopancreas. *J. Mar. Biol. Ass. UK* **60**, 891-907. doi:10.1017/S0025315400041977

Jiang, R., Liu, H., Liu, M., Tian, J., Huang, Q., Huang, H., Wen, Y., Cao, Q.-Y., Zhang, X. and Wei, Y. (2017). A facile one-pot Mannich reaction for the construction of fluorescent polymeric nanoparticles with aggregation-induced emission feature and their biological imaging. *Mater. Sci. Eng. C. Mater. Biol. Appl.* **81**, 416-421. doi:10.1016/j.msec.2017.08.048

Leary, S., Underwood, W., Anthony, R., Cartner, S., Corey, D., Grandin, T., Greenacre, C., Gwaltney-Brant, S., McCrackin, M. A., Meyer, R. et al. (2013). *AVMA Guidelines for the Euthanasia of Animals*, 2013 edn. Schaumburg, IL: American Veterinary Medical Association.

Lightner, D. V. (1988). Vibrio disease of penaeid shrimp. In *Disease Diagnosis and Control in North American Marine Aquaculture and Fisheries Science* (ed. C. J. Sinderman and V. Lightner), pp. 42-47. Amsterdam: Elsevier.

Lima, J. F., Garcia, J. S. and Tavares, M. (2016). Foregut morphology of *Macrobrachium carcinus* (Crustacea, Decapoda, Palaemonidae). *Acta. Amaz.* **46**, 209-218. doi:10.1590/1809-4392201501214

Lin, F.-Y. (1996). Structure of the gland filters in the pyloric stomach of *Penaeus japonicus* (Decapoda: Penaeidae). *J. Crustacean. Biol.* **16**, 515-521. doi:10.2307/1548741

Lin, F.-Y. (2000). Scanning electron microscopic observations on the gland filters of the pyloric stomach of *Penaeus monodon* and *Metapenaeus ensis* (Decapoda, Penaeidae). *Crustaceana* **73**, 163-174. doi:10.1163/156854000504237

Martin, G. G. and Hose, J. E. (2010). Functional anatomy of penaeid shrimp. In *The Shrimp Book* (ed. V. Alday-Sanz), pp. 47-72. Nottingham: Nottingham University Press.

McGaw, I. J. and Curtis, D. L. (2013). A review of gastric processing in decapod crustaceans. *J. Comp. Physiol. B* **183**, 443-465. doi:10.1007/s00360-012-0730-3

Meiss, D. E. and Norman, R. S. (1977). Comparative study of the stomatogastric system of several decapod Crustacea. I. Skeleton. *J. Morphol.* **152**, 21-53. doi:10.1002/jmor.1051520103

Muhammad, F., Zhang, Z.-F., Shao, M.-Y., Dong, Y.-P. and Muhammad, S. (2012). Ontogenesis of digestive system in *Litopenaeus vannamei* (Boone, 1931) (Crustacea: Decapoda). *Ital. J. Zool.* **79**, 77-85. doi:10.1080/11250003.2011.590534

Ooms-Wilms, A. L., Postema, G. and Gulati, R. D. (1995). Evaluation of bacterivory of Rotifera based on measurements of *in situ* ingestion of fluorescent particles, including some comparisons with Cladocera. *J. Plankton. Res.* **17**, 1057-1077. doi:10.1093/plankt/17.5.1057

Pollack, J., Lawrence, A. L. and Feller, R. J. (2006). Practical equivalence of laboratory and field measurements of gut passage time in two penaeid shrimp species. *Mar. Ecol. Prog. Ser.* **309**, 221-231. doi:10.3354/meps309221

Schaefer, N. (1970). The functional morphology of the foregut of three species of Decapod Crustacea: *Cyclograpsus punctatus* Milne-Edwards, *Diogenes brevirostris* Stimpson, and *Upogebia africana* (Ortmann). *Zoologica. Africana.* **5**, 309-326. doi:10.1080/00445096.1970.11447399

Simon, C. J. (2009). Digestive enzyme response to natural and formulated diets in cultured juvenile spiny lobster, *Jasus edwardsii*. *Aquaculture* **294**, 271-281. doi:10.1016/j.aquaculture.2009.06.023

Simon, C. J., Carter, C. G. and Battaglene, S. C. (2012). Development and function of the filter-press in spiny lobster, *Sagmariasus verreauxi*, phyllosoma. *Aquaculture* **370-371**, 68-75. doi:10.1016/j.aquaculture.2012.10.003

Song, Y.-L., Cheng, W. and Wang, C.-H. (1993). Isolation and characterization of *Vibrio damsela* infectious for cultured shrimp in Taiwan. *J. Invertebr. Pathol.* **61**, 24-31. doi:10.1006/jipa.1993.1005

Storch, V., Bluhm, B. A. and Arntz, W. E. (2001). Microscopic anatomy and ultrastructure of the digestive system of three Antarctic shrimps (Crustacea: Decapoda: Caridea). *Polar. Biol.* **24**, 604-614. doi:10.1007/s003000100261

Thitamadee, S., Prachumwat, A., Srisala, J., Jaroenlak, P., Salachan, P. V., Sritunyalucksana, K., Flegel, T. W. and Itsathitphaisarn, O. (2016). Review of current disease threats for cultivated penaeid shrimp in Asia. *Aquaculture* **452**, 69-87. doi:10.1016/j.aquaculture.2015.10.028

Tzuc, J. T., Escalante, D. R., Herrera, R. R., Gaxiola Cortés, G. and Ortiz, M. L. A. (2014). Microbiota from *Litopenaeus vannamei*: digestive tract microbial community of Pacific white shrimp (*Litopenaeus vannamei*). *SpringerPlus* **3**, 280-290. doi:10.1186/2193-1801-3-280

Wade, N. M., Bourne, N. and Simon, C. J. (2018). Influence of marker particle size on nutrient digestibility measurements and particle movement through the digestive system of shrimp. *Aquaculture* **491**, 273-280. doi:10.1016/j.aquaculture.2018.03.039

Wallis, E. J. and Macmillan, D. L. (1998). Foregut morphology and feeding strategies in the Syncarid Malacostracan *Anaspides tasmaniae*: correlating structure and function. *J. Crustacean. Biol.* **18**, 279-289. doi:10.2307/1549321

Watts, A. J. R., Lewis, C., Goodhead, R. M., Beckett, S. J., Moger, J., Tyler, C. R. and Galloway, T. S. (2014). Uptake and retention of microplastics by the shore crab *Carcinus maenas*. *Environ. Sci. Technol.* **48**, 8823-8830. doi:10.1021/es501090e

Woods, C. M. C. (1995). Functional morphology of the foregut of the spider crab *Notomithrax ursus* (Brachyura: Majidae). *J. Crustacean. Biol.* **15**, 220-227. doi:10.2307/1548950